Published in final edited form as:
Proc Am Control Conf. 2014 ; 2014: 443–450. doi:10.1109/ACC.2014.6858649.

Local E-optimality Conditions for Trajectory Design to Estimate Parameters in Nonlinear Systems

Andrew D. Wilson and **Todd D. Murphey**
The Department of Mechanical Engineering, Northwestern University, 2145 Sheridan Road, Evanston, IL 60208, USA

Andrew D. Wilson: awilson@u.northwestern.edu; Todd D. Murphey: t-murphey@northwestern.edu

Abstract

This paper develops an optimization method to synthesize trajectories for use in the identification of system parameters. Using widely studied techniques to compute Fisher information based on observations of nonlinear dynamical systems, an infinite-dimensional, projection-based optimization algorithm is formulated to optimize the system trajectory using eigenvalues of the Fisher information matrix as the cost metric. An example of a cart-pendulum simulation demonstrates a significant increase in the Fisher information using the optimized trajectory with decreased parameter variances shown through Monte-Carlo tests and computation of the Cramer-Rao lower bound.

I. Introduction

The design of trajectories for the experimental identification of parameters in dynamic systems is an important problem in a variety of fields ranging from robotics to biology to chemistry and beyond. With more accurate models, the performance and tuning of controllers can be radically improved. For nonlinear dynamical systems, the trajectory is constrained to a nonlinear set of equations of motion which leads to challenges in parameter estimation. Additionally, since the trajectories evolve on a continuous-time domain, it is important to ensure that the dynamics are satisfied along the entire time domain of any synthesized trajectory.

A variety of estimation techniques are used in practice, including Kalman filtering, maximum likelihood estimators, and Monte-Carlo estimators to name a few [1-3]. The focus of this paper will lie solely in the area of estimating static model parameters in nonlinear dynamical systems. A widely used method of estimating these types of parameters is through a maximum likelihood estimation technique known as batch least-squares estimation [3].

The batch least-squares method compares a set of measurements taken along the evolution of a trajectory to predicted observations of the system using the model equations and estimates of the parameters. This comparison is made using the method of least-squares along the trajectory, and a new update to the parameter estimate is then calculated.

II. Related Work

The design of the experimental trajectory is of particular importance to maximize the amount of information gained from the parameter estimation task. A large amount of literature on optimal experimental design exists in the fields of biology [4-6], chemistry [7], and systems [8-11].

A common metric used in the area of experimental design that will also be a key metric in this paper is the Fisher information matrix computed from observations of the system trajectory [12]. Metrics based on Fisher information are used as cost functions in many optimization problems including work by Swevers on “exciting” trajectories [13]. This work, as well as related works [14], [15], synthesize trajectories for nonlinear systems that can be recast as linear systems with respect to the parameters.

Further research has resulted in optimal design methods for general nonlinear systems. In work by Emery [16], similar least-squares and maximum likelihood estimation techniques are combined with Fisher information to optimize the dynamic experiment. In this case and a number of others, the dynamics are solved as a discretized, constrained optimization problem [17], [18].

To avoid a discretization of the dynamics of the continuous system, a class of methods has been developed which relies on sets of basis functions to synthesize an optimal control input to the system [19-21]. This method allows the full trajectory to be optimized on a continuous-time domain; however, the optimization is still subject to a finite set of basis function coefficients.

The main contribution of this paper is the formulation of an infinite-dimensional, projection-based optimization algorithm which maximizes the information gained from observations along the dynamic trajectory. The projection-based algorithm was originally designed for optimal trajectory tracking problems [22], [23]; however, this paper extends the algorithm to include a non-Bolza cost function, maximizing the information gained by observations of the dynamic trajectory. This formulation results in a method that preserves the continuous-time dynamics using variational perturbations to the input and trajectory to find an optimal solution.

This paper is organized as follows: Section III introduces the estimation concepts required to compute the Fisher information matrix for the system. Section IV derives the required cost function and equations necessary to optimize the trajectory over the Fisher information. Finally, an example of the optimization algorithm is provided for a cart-pendulum system in simulation.

III. Least-Squares Estimation

This paper will assume that a predefined number of model parameters are being estimated from a series of state measurements taken along a dynamic system’s trajectory evolution. To provide background for the trajectory optimization objective function, which will be

presented in the next section, the estimation procedure will first be outlined. The dynamic model of the system is defined as

$$\dot{x}(t) = f(x(t), u(t), \theta) \quad (1)$$

where $x \in \mathbb{R}^n$ defines the system states, $u \in \mathbb{R}^m$ defines the inputs to the system, and $\theta \in \mathbb{R}^p$ defines the set of model parameters that will be estimated. For the purpose of this paper, all states will be assumed to be observable for the estimation algorithm.

When running an experiment, a predefined trajectory, $x(t)$, is executed, and measurements of the state are taken during the evolution of the experiment. We will assume that the trajectory has a finite time horizon, and a fixed number of observations are made. This assumption commonly occurs for fixed frequency sampling of sensors over a fixed time horizon in an experimental setup. Using the collected measurements, least-squares estimation of the parameter set can be performed using a Newton-Raphson search method. The objective of the least-squares estimator can be rewritten as

$$\widehat{\theta} = \arg \min_{\theta} \lambda(\theta)$$

where

$$\lambda(\theta) = \sum_{i}^{h} (\tilde{x}(t_i) - x(t_i))^T \cdot \sum^{-1} \cdot (\tilde{x}(t_i) - x(t_i)).$$

$x(\tilde{t}_i)$ is the observed state at the i^{th} time-point of h measurements and $\Sigma \in \mathbb{R}^{n \times n}$ is the covariance matrix associated with the sensor measurement error.

Given this minimization problem, the Newton-Raphson iterator is given by

$$\hat{\theta}_{k+1} = \hat{\theta}_k - \left[\nabla^2_{\theta} \lambda(\theta)\right]^{-1} \nabla_{\theta} \lambda(\theta).$$

A. Fisher Information

The Fisher information matrix quantifies the amount of information a set of observations contains about a set of unknown parameters. Assuming that the measurement noise of the system is normally distributed, the Fisher information matrix for the linear estimator is given by

$$I(\theta) = \sum_{i}^{h} \nabla_{\theta} x(t_i) \cdot \sum^{-1} \cdot \nabla_{\theta} x(t_i)^T.$$

Since $I(\theta) \in \mathbb{R}^{n \times n}$, an appropriate metric must be chosen which involves the Fisher information matrix. There is a significant amount of literature on different types of mapping choices [4], [16], [17]; however, this paper will restrict itself to the design choice of E-

optimality. This choice of mapping attempts to improve the worst-case variances of the parameter set by maximizing the minimum eigenvalue of the Fisher information matrix.

Given this choice of mapping, the objective function for the trajectory optimization includes the inverse of the minimum eigenvalue as well as cost on the control effort. Additionally, a trajectory cost may be added to keep optimal trajectories in the neighborhood of the initial trajectory. The details of the trajectory optimization cost and routine will be presented in the following section.

IV. Nonlinear Trajectory Optimization

A. Objective Function

The trajectory optimization problem described in the previous section will now be formally defined. The objective function, J is dependent on the eigenvalues of the Fisher information matrix, $I(\theta)$. Since our optimization method requires a continuous cost function, the maximization of the information matrix needs to be cast into an appropriate continuous analogue. To satisfy this condition, the information equation will be written as

$$\tilde{I}(\theta) = \int_{t_0}^{t_f} \nabla_\theta x(t) \cdot \sum^{-1} \cdot \nabla_\theta x(t)^T dt. \quad (2)$$

Assuming that observations are taken regularly along the entire trajectory, the optimal trajectory $x^*(t)$ maximizing the eigenvalues of the continuous $\tilde{I}(\theta)$ will approximately optimize the eigenvalues of the sampled $I(\theta)$. As the sampling rate increases, the values of $\tilde{I}(\theta)$ and $I(\theta)$ will converge.

If observations do not take place along the entire trajectory and the times samples are measured along the trajectory are predetermined, a weighting function can be added to $\tilde{I}(\theta)$ to ensure that sensitivity is maximized in the sampled areas of the trajectory. However, if the observation time is not predetermined, the sensitivity along the entire trajectory will be maximized using $\tilde{I}(\theta)$.

The optimization objective function will therefore be given by

$$J = \frac{Q_p}{\lambda_{min}} + \frac{1}{2}\int_{t_0}^{t_f} \Big[(x(t) - x_d(t))^T \cdot Q_\tau \cdot (x(t) - x_d(t)) + u(t)^T \cdot R_\tau \cdot u(t) \Big] dt \quad (3)$$

where λ_{min} is the minimum eigenvalue of $\tilde{I}(\theta)$, Q_p is the information weight, $x_d(t)$ is a reference trajectory, Q_τ is a trajectory tracking weighting matrix, and R_τ is a control effort weighting matrix.

The various weights allow for design choices in the optimal trajectory that is obtained. The control weight is required to maintain a convex optimization problem and must be a positive definite matrix. Increasing this weight will result in less aggressive trajectories, most likely decreasing the obtained information. Using a reference trajectory allows for an optimal solution that remains in the neighborhood of a known trajectory.

To minimize the objective function given by (3), an optimal control algorithm is formulated using an infinite dimensional, projection-based approach. The technique is founded on the approach detailed in [22], but is extended in this paper to allow for a cost function in the form of (3).

B. Extended Dynamics Constraints

For the optimization of the system trajectory, the objective function must be minimized while satisfying the governing dynamic equations of the system. The nonlinear system dynamics are given by (1).

The optimal control algorithm traditionally was formulated for trajectory tracking problems where the objective function is explicitly a function of the system states. However, given the formulation of the objective function in the previous section, the cost depends on $\nabla_\theta x(t)$. The Jacobean along the trajectory can be calculated by first writing $x(t)$ in its integral form,

$$x(t) = x_0 + \int_{t_0}^{t_f} f(x(t), u(t), \theta)\, dt.$$

Calculating the Jacobean with respect to θ, yields

$$\nabla_\theta x(t) = \int_{t_0}^{t_f} D_x f(x(t), u(t), \theta)^T \nabla_\theta x(t) + D_\theta f(x(t), u(t), \theta)^T dt.$$

If the above equation is now differentiated with respect to time, a new ODE can be written in terms of the Jacobean of the state with respect to θ,

$$\dot{\psi}(t) = D_x f(x(t), u(t), \theta)^T \dot{\psi}(t) + D_\theta f(x(t), u(t), \theta)^T \quad (4)$$

where

$$\psi(t) = \nabla_\theta x(t).$$

Since the equation for the Jacobean denoted by $\psi(t)$ is, in effect, an additional equation that must be satisfied by the optimal trajectory $x^*(t)$, $\psi(t)$ will be appended to the state vector as an additional dynamic constraint. This will allow for variations on $\psi(t)$ to be made directly in the optimization algorithm followed by a projection step to satisfy both $x(t)$ and $\psi(t)$.

For convenience, $\bar{x}(t) = (x(t), \psi(t))$ will define the expanded states and $\bar{\eta}(t) = (\bar{x}(t), u(t))$ defines a feasible curve on the trajectory manifold, T.

C. Projection Operator

The minimization of (3) is subject to the dynamics constraints given by (1) and (4). This constrained optimization can be relaxed by calculating a descent direction using an unconstrained iterate followed by a projection of the descent direction onto the dynamics constraints as detailed in [22]. The projection operator uses a stabilizing feedback law to

take a feasible or infeasible trajectory, defined by $\xi(t) = (\bar{\alpha}(t), \mu(t))$ and maps it to a feasible trajectory, $\eta(t)$.

The projection operator used in this paper is given by

$$P(\xi(t)): \begin{cases} u(t) = \mu(t) + K(t)(\overline{\alpha}(t) - \overline{x}(t)) \\ \dot{x}(t) = f(x(t), u(t)) \\ \dot{\psi}(t) = D_x f(x,u,\theta)^T \psi(t) + D_\theta f(x,u,\theta)^T. \end{cases}$$

The feedback gain, $K(t)$ can be optimized as well by solving an additional linear quadratic regulation problem. Details of the optimal gain problem can be found in [22].

With the addition of the projection operator, the optimization problem can be reformulated as an unconstrained problem of the form

$$\arg \min_{\xi(t)} J(P(\xi(t))).$$

This allows variations of the trajectory to be calculated free of the constraint of maintaining feasible dynamics; however, the solution is projected to a feasible trajectory at each iteration of the optimization algorithm.

D. Optimization Routine

The optimal control problem is solved using a gradient descent technique. In order to apply the iterative method, a descent direction must be defined for each iteration of the algorithm. The descent direction, $\zeta_i(t)$ is given by

$$\zeta_i(t) = \arg \min_{\zeta_i(t)} DJ(P(\xi_i(t))) \circ \zeta_i(t) + \frac{1}{2} \langle \zeta_i(t), \zeta_i(t) \rangle \quad (5)$$

where $\zeta_i(t) \in T_{\xi_i} T$, i.e., the descent direction lies in the tangent space of the trajectory manifold at the current iteration. The components of the descent direction are given by $\zeta_i = (z(\bar{t}), \upsilon(t))$ where $z(\bar{t})$ is the perturbation to the extended state and $\upsilon(t)$ is the perturbation to the control.

The solution to (5) results in a descent direction for the optimal control problem (3) and an appropriate Armijo step of the projection, $P(\xi_i(t) + \gamma_i \zeta_i)$ provides a feasible trajectory solution assuming that the step size γ_i satisfies a sufficient decrease condition.

The basic algorithm is shown in Algorithm 1. The descent direction is found by defining a local LQR optimization problem at each iteration of the trajectory [24]. The following section will cover the setup and structure of this LQR problem. Sufficient decrease is satisfied by an Armijo line search on the solution which is projected onto the trajectory manifold [25]. After the steepest descent condition is satisfied, the updated trajectory becomes the seed for the next iteration of the optimal control algorithm.

Algorithm 1 Trajectory Optimization

Initialize $\xi_0 \in T$, tolerance ε

while $DJ(\xi_i(t)) \circ \zeta_i > \varepsilon$ **do**

Calculate descent, ζ_i:

$$\zeta_i = \arg\min_{\zeta_i(t)} DJ\left(P\left(\xi_i(t)\right)\right) o\zeta_i + \frac{1}{2}\langle\zeta_i, \zeta_i\rangle$$

Compute γ_i with Armijo backtracking search

Project onto dynamics constraints:

$\xi_{i+1}(t) = P(\xi_i(t) + \gamma_i\zeta_i)$

$i = i + 1$

end while

E. Solving the LQR Problem

To find a descent direction for the optimal control algorithm, the LQR problem must first be formulated. As given shown in (5), the descent direction depends on the linearization of the cost function, $DJ(P(\zeta_i(t)))$ and the local quadratic model, $\frac{1}{2}\langle\zeta_i(t), \zeta_i(t)\rangle$. The following subsections present the formulations for these two quantities as well as the linearization of the dynamics which constrain the descent direction.

1) Cost Function Linearization—The linearization of the cost function, $DJ(P(\zeta_i(t)))$ will be found by taking the directional derivative of (3) with respect to the extended states, $x(\bar{t})$, and the control vector, $u(t)$.

The derivative of (3) with respect to x yields

$$a(t) = \frac{\partial J}{\partial \bar{x}} = -\frac{1}{\lambda_{min}^2}\frac{\partial \lambda_{min}}{\partial \bar{x}} + \int_{t_0}^{t_f}\left[(x(t) - x_d(t))^T \cdot Q_\tau\right] dt. \quad (6)$$

Since the cost function involves the eigenvalues of $\tilde{I}(\theta)$, this linearization requires a method of handling derivatives of eigenvalues. An equation for derivatives of eigenvalues was formalized by Nelson [26]. Given an eigensystem of the form

$$AX = X\Lambda$$

where Λ is a diagonal matrix of eigenvalues, ($\lambda_1, \lambda_2, \ldots\lambda_n$), and X is the associated matrix of eigenvectors, the derivative of one eigenvalue is given by

$$D_x\lambda_k = y_k^T \cdot D_x A \cdot \upsilon_k$$

where y_k is the left eigenvector and υ_k is the right eigenvector associated with λ_k.

Using this result, $\frac{\partial \lambda_{min}}{\partial \overline{x}}$ from (6) can be calculated. Taking the derivative of the eigenvalue of $\tilde{I}(\theta)$ from (2) with respect to the extended state yields

$$\frac{\partial \lambda_i}{\partial \overline{x}} = y_i^T \frac{\partial}{\partial \overline{x}} \left(\int_{t_0}^{t_f} \nabla_\theta x(t) \cdot \sum^{-1} \cdot \nabla_\theta x(t)^T dt \right) \upsilon_i$$

where *i* denotes the index of the minimum eigenvalue and eigenvector. Since the partial derivative and eigenvectors are not time dependent, the equation can be rewritten as the running cost over the derivative of the outer product of the Jacobeans,

$$\frac{\partial \lambda_i}{\partial \overline{x}} = \int_{t_0}^{t_f} y_i^T \frac{\partial}{\partial \overline{x}} \left(\nabla_\theta x(t) \cdot \sum^{-1} \cdot \nabla_\theta x(t)^T \right) \upsilon_i \, dt.$$

The last step in computing the extended state linearization of the cost function is calculating the derivative of the outer product of the Jacobeans, $\frac{\partial}{\partial \overline{x}} = (\nabla_\theta x(t) \nabla_\theta x(t))$. Given that $\nabla_\theta x(t)$ is included in the extended state, $x(\bar{t})$, the partial derivative of the outer product is straightforward. The matrix representation of the derivative is given by

$$\frac{\partial}{\partial \overline{x}} = \left(\nabla_\theta x(t) \cdot \sum^{-1} \cdot \nabla_\theta x(t)^T \right) = \begin{bmatrix} \{0\}^{n \times p \times n} \\ 2 \nabla_\theta x(t) \cdot \sum^{-1} \cdot E \end{bmatrix}$$

where *E* is an identity-like tensor of the form

$$E_{i,j,k,l} = \delta_{i,k} \delta_{j,l}$$

with $\delta_{,}$. as the Kronecker delta function.

Given the cost function (3), the linearization has been defined in terms of the expanded state, $x(\bar{t})$. Additionally, the linearization with respect to the control $u(t)$ is needed. $\frac{\partial J}{\partial u}$ is much simpler since only the control cost term is directly dependent on the control. Therefore, the linearization is given by

$$b(t) = \frac{\partial J}{\partial u} = \int_{t_0}^{t_f} \left[u(t)^T \cdot R_\tau \right] dt. \quad (7)$$

These linearization terms are evaluated using the state and control at each point in time along the trajectory.

2) Quadratic Model—The second required component of the LQR problem is defining the inner product, $\frac{1}{2} \langle \zeta_i, \zeta_i \rangle$. For this paper, we will choose a simple quadratic model related to the extended state and control inputs. This will be defined as

$$\frac{1}{2}\left\langle \zeta_i, \zeta_i \right\rangle = \int_{t_0}^{t_f} \frac{1}{2} \overline{z}(t)^T Q(t)\, \overline{z}(t) + \upsilon(t)^T R(t)\, \upsilon(t)\, dt$$

where matrices $Q(t)$ and $R(t)$ are weighting matrices for the local quadratic model approximation. Design of these weighting matrices can lead to faster convergence of the optimal control algorithm depending on the specific problem.

3) Dynamics Linearization—The final step required to set up the LQR problem is to calculate linearizations of the dynamics. Since the original dynamics for the system are nonlinear, linearized dynamics are used as an approximation for the steepest descent calculation and then the projection operator projects the step back onto the nonlinear dynamics.

The descent direction, ζ_i, will satisfy the linear constraint ODE given by

$$\dot{\overline{z}}_i(t) = A(t)\, \overline{z}_i(t) + B(t)\, \upsilon_i(t)$$

where $A(t)$ is the linearization of the nonlinear dynamics given by (1) and (4) with respect to $x(\bar{t})$, and $B(t)$ is the linearization with respect to $u(t)$. The linearization, $A(t)$, of the dynamics with respect to the extended state, $x(\bar{t})$, is given by

$$\begin{aligned} A(t) &= \begin{bmatrix} \frac{\partial \dot{x}}{\partial x} & \frac{\partial \dot{x}}{\partial \psi} \\ \frac{\partial \dot{\psi}}{\partial x} & \frac{\partial \dot{\psi}}{\partial \psi} \end{bmatrix} \\ &= \begin{bmatrix} D_x f(\cdot) & \{0\} \\ D_x^2 f(\cdot) \cdot \psi(t) + D_x D_\theta f(\cdot) & D_x f(\cdot) \cdot E \end{bmatrix}. \end{aligned}$$

Additionally, the linearization of the dynamics with respect to the control input, $u(t)$, is required. This linearization matrix, $B(t)$, is given by

$$\begin{aligned} B(t) &= \begin{bmatrix} \frac{\partial \dot{x}}{\partial u} \\ \frac{\partial \dot{\psi}}{\partial u} \end{bmatrix} \\ &= \begin{bmatrix} D_u f(\cdot) \\ D_u D_x f(\cdot) \cdot \psi(t) + D_u D_\theta f(\cdot) \end{bmatrix}. \end{aligned}$$

Given the cost function linearization and quadratic model, the LQR problem which solves for the descent direction (5) can be written as

$$\begin{aligned} \arg\min_{\zeta(t)} = & \int_{t_0}^{t_f} a(t)^T \overline{z}(t) + b(t)^T \upsilon(t) \\ & + \tfrac{1}{2} \overline{z}(t)^T Q(t)\, \overline{z}(t) + \tfrac{1}{2} \upsilon(t)^T R(t)\, \upsilon(t)\, dt \end{aligned} \tag{8}$$

such that

$$\dot{\bar{z}}(t) = A(t)\,\bar{z}(t) + B(t)\,v(t)$$

where $a(t) = \frac{\partial J}{\partial \bar{x}}$, $b(t) = \frac{\partial J}{\partial u}$ and $A(t)$ and $B(t)$ are the linearizations of the system dynamics. The problem is therefore reduced to solving this LQR problem iteratively to find directions of steepest descent. The solution to the LQR descent problem can then be solved using the known Riccati differential equations [22]. Since this descent direction is based on the linearized dynamics, the projection operator must be applied to ensure the dynamics constraints are satisfied. This process is iteratively repeated until convergence is achieved as shown in Algorithm 1.

V. Simulation Example

To demonstrate the procedure and use of optimizing the Fisher information for a dynamic system, a simulation of a cart-pendulum system is considered. The system has two degrees of freedom, ($s(t)$, $\varphi(t)$), where $s(t)$ is the horizontal displacement of the cart and $\varphi(t)$ is the rotational angle of the pendulum as seen in Fig. 1.

A horizontal control force can be applied in either direction to the cart with positive force to the right and a torque due to rotational friction is added to the pendulum joint. The Lagrangian for this system is given by

$$L = \frac{1}{2}(M+m)\,\dot{s}^2 - m\ell\dot{s}\dot{\varphi}\cos\varphi + \frac{1}{2}m\ell^2\dot{\varphi}^2 - mg\ell\cos\varphi,$$

and the equations of motion for the cart-pendulum can be derived with the Euler-Lagrange equations given by

$$\frac{\partial L}{\partial s} - \frac{d}{dt}\frac{\partial L}{\partial \dot{s}} = u(t)\,;\ \frac{\partial L}{\partial \phi} - \frac{d}{dt}\frac{\partial L}{\partial \dot{\phi}} = -c\dot{\phi}(t)\,,$$

where M is the cart mass, m is the pendulum mass, ℓ is the pendulum length, and c is the viscous friction parameter. The full equations will not be derived here; however, the results are easily obtained.

A. Simulation Parameters

The goal for this trajectory optimization simulation will be to estimate three parameters given noisy measurements of the full state of the system. The three parameters will be the mass of the pendulum, m, the length of the pendulum, ℓ, and the friction coefficient, c.

An experimental measurement of the trajectory is simulated by sampling the trajectory of the system given the current estimate of parameters at a discrete number of points. Additive noise is then added to each sample which results in a simulated set of noisy measurements that will be used for the subsequent optimization routine. For this simulation example, a 4 second trajectory will be measured with a fixed sampling rate of 100 Hz. The uncertainty of

each state measurement will be normally distributed with zero mean and a standard deviation, $\sigma = 0.05$.

An initial control input is chosen as shown in Fig. 2c. An initial guess of the parameters, $\theta = \{m, \ell, c\}$, is also chosen as well as the actual deterministic parameter set. The parameters and estimates used to initialize the optimization are:

$$Actual{:}m{=}2.0kg,\ \ell{=}1.0\mathrm{m},\ c{=}1.0\mathrm{Ns/m}$$
$$Guess{:}m{=}2.5kg,\ \ell{=}1.4m,\ c{=}1.4\mathrm{Ns/m}$$

The cart mass will be assumed to be known and fixed at 1.0 kg.

B. Optimization Results

The optimization was run until the convergence criterion $|DJ(\xi(t)) \circ \zeta| < 10^{-2}$ was satisfied. The comparison of initial and optimized trajectories can be seen in Fig. 2. By examining Fig. 2d, it is clear that the optimized trajectory dramatically improves the amount of Fisher information as the trajectory evolves in time. This increase in information is due to the fact that the system is being excited in a way that allows the parameters to be observed more accurately. As an intuitive example, the increased oscillation of the pendulum, seen in Fig. 2b, allows a better estimate of the friction parameter, *c*, to be made since the system is subject to greater frictional torques.

In terms of the optimization cost, the initial and optimized eigenvalues of $\tilde{I}(\theta)$ and *J* are listed in Table I. The results show that the minimum eigenvalue, λ_3, increases by over a factor of 100. Additionally, the other eigenvalues also increase, though not included directly in the cost function. The results can also be visualized through the phase-space representation of the sensitivities, $\psi(t)$. Fig. 3 shows the phase plot of $\nabla_c \varphi(t)$ which indicates that the optimized trajectory maximizes the Fisher information by quickly increasing the sensitivity of the system throughout the trajectory.

Examining the plots of the optimized trajectory, it is clear that more information is gained by oscillating the pendulum back and forth. In particular, more information about the torsional friction parameter, *c*, is gained by increasing the oscillation. This observation leads to a hypothesis that the cost function and optimization may be driven strongly by information concerning the friction parameter.

This hypothesis is confirmed by examining the eigenvector associated with λ_3. The eigenvector is {0.0060018, 0.066900, 0.99774}, which indicates that the largest initial direction of the eigenvalue and therefore the optimization is *c*. This analysis validates the qualitative observations made about the optimization results; however, another important test is to confirm that the variance of the parameter estimate indeed decreases with the increased information.

C. Monte-Carlo Analysis

To quantitatively compare the variance of the parameter estimates for both trajectories, a Monte-Carlo test was performed with both the initial and optimized trajectories using the

batch-least squares estimation method. The parameter estimation routine was run 1500 times for each of the trajectories. For each trial, a new set of sampled random noise was used.

A histogram of the distribution of estimated values of the friction parameter, *c* can be seen in Figure 4. The covariance matrix for all three parameters computed from the Monte-Carlo data as well as the Fisher information matrix, $I(\theta)$ for each trajectory can be seen in Table II.

The results from the Monte-Carlo tests confirm that the Fisher information significantly increases when the optimized trajectory is used in estimating the model parameters. Additionally, this increase in information leads to a significant decrease in the variance of the parameter estimates. In particular, the variance of the friction coefficient, *c* decreases from 0.0595 Ns/m to 0.000170 Ns/m.

D. Cramer-Rao Lower Bound

The final comparison that will be made with the results obtained from the simulation is with regard to the Cramer-Rao bound. Since it is assumed that the measurement noise is normally distributed with zero mean and the estimation method is least-squares, the Cramer-Rao bound on the variance simply states that

$$cov_\theta(\beta) \geq I(\theta)^{-1}$$

where β is the batch least-squares estimator [27]. This places an absolute lower bound on the variance of the parameter estimate that can be obtained using the batch least-squares estimator or other unbiased estimator.

Table III lists the covariance bounds for the initial and optimized trajectories. The covariance of the initial trajectory is clearly subject to a higher bound than that of the optimized trajectory. Due to round-off and other numerical errors in the algorithms and Monte-Carlo simulations, the covariance of the Monte-Carlo estimates is higher than the lower bound; however, overall remains quite close to the predicted best-case variance estimates according to the Cramer-Rao bound.

VI. Conclusion

This paper presented a method of performing an optimization of the Fisher information subject to the dynamics of a nonlinear system. By extending an infinite-dimensional projection-based trajectory optimization algorithm, the continuous-time dynamics could be preserved throughout the optimization, and variations on the input and trajectory were projected onto the trajectory manifold, T.

The results of the cart-pendulum simulation show that this optimization routine results in an increase in the minimum eigenvalue of the Fisher information as well as a decrease in the covariance of the estimated parameters subject to the Cramer-Rao lower bound. Future work related to the optimization approach involves exploring bounds on the convergence rates including adding second-order information to the optimization algorithm. Additionally, experimental trials are planned to compare simulation data to physical measurements.

Acknowledgments

This material is based upon work supported by the National Institute of Health under NIH R01 EB011615 and by the National Science Foundation under Grant CMMI 1334609. Any opinions, findings, and conclusions or recommendations expressed in this material are those of the author(s) and do not necessarily reflect the views of the National Science Foundation.

References

1. Kalman RE, Bucy RS. New Results in Linear Filtering and Prediction Theory. J of Basic Eng. 1961; 83:95–108.
2. Ljung L, L. System Identification: Theory for the User. 2. Prentice Hall; 1999.
3. Bar-Shalom, Y.; Li, XR.; Kirubarajan, T. Estimation with Applications to Tracking and Navigation. New York: John Willey and Sons; 2001.
4. Faller D, Klingmuller U, Timmer J. Simulation Methods for Optimal Experimental Design in Systems Biology. SIMULATION. Dec; 2003 79(12):717–725.
5. Baltes M, Schneider R, Sturm C, Reuss M. Optimal experimental design for parameter estimation in unstructured growth models. Biotechnology Progress. 1994; 10(5):480–488.
6. Oliver Lindner P, Hitzmann B. Experimental design for optimal parameter estimation of an enzyme kinetic process based on the analysis of the Fisher information matrix. J of Theoretical Biology. Jan; 2006 238(1):111–123.
7. Franceschini G, Macchietto S. Model-based design of experiments for parameter precision: State of the art. Chemical Engineering Science. 2008; 63(19):4846–4872.
8. Dietrich, F.; Raatz, A.; Hesselbach, J. A-priori Fisher information of nonlinear state space models for experiment design. 2010 IEEE Int Conf on Robotics and Automation; 2010. p. 3698-3702.
9. Martensson J, Rojas CR, Hjalmarsson H. Conditions when minimum variance control is the optimal experiment for identifying a minimum variance controller. Automatica. 2011; 47(3):578–583.
10. Joshi S, Boyd S. Sensor selection via convex optimization. IEEE Trans on Signal Processing. 2009; 57(2):451–462.
11. Gevers M, Bombois X, Hildebrand R, Solari G. Optimal experiment design for open and closed-loop system identification. Communications in Information and Systems. 2011; 11(3):197–224.
12. Lehmann, EL.; Casella, G. Theory of Point Estimation. New York: Springer; 1998.
13. Swevers J, Ganseman C, Tkel BD, De Schutter J, Van Brussel H. Optimal robot excitation and identification. IEEE Trans Robot Automat. May.1997 13:730–740.
14. Armstrong B. On finding exciting trajectories for identification experiments involving systems with nonlinear dynamics. Int J Robot Res. 1989; 8(6):28–48.
15. Gautier M, Khalil W. Exciting trajectories for the identification of base inertial parameters of robots. Int J Robot Res. 1992; 11(4):362–375.
16. Emery A, Nenarokomov A. Optimal experiment design. Measurement Science and Tech. 1999; 9(6):864–876.
17. Mehra R. Optimal input signals for parameter estimation in dynamic systems-Survey and new results. IEEE Trans on Automatic Control. Dec; 1974 19(6):753–768.
18. Vincent TL, Novara C, Hsu K, Poolla K. Input design for structured nonlinear system identification. Automatica. Jun; 2010 46(6):990–998.
19. Wahlberg, B.; Hjalmarsson, H.; Annergren, M. On optimal input design in system identification for control. 49th IEEE Conf on Decision and Control; 2010. p. 5548-5553.
20. Wu W, Zhu S, Wang X, Liu H. Closed-loop dynamic parameter identification of robot manipulators using modified Fourier series. Int J Adv Robot Sys. 2012; 9(29)
21. Rackl, W.; Lampariello, R.; Hirzinger, G. Robot excitation trajectories for dynamic parameter estimation using optimized B-splines. 2012 IEEE Conf Robotics and Automation; May. 2012 p. 2042-2047.
22. Hauser, J. A projection operator approach to optimization of trajectory functionals. IFAC world congress; Barcelona, Spain. 2002.

23. Hauser, J.; Meyer, DG. The trajectory manifold of a nonlinear control system. 37th IEEE Conf on Decision and Control; 1998. p. 1034-1039.
24. Anderson, BDO.; Moore, JB. Optimal Control: Linear Quadratic Methods. Prentice-Hall; 1989.
25. Armijo L. Minimization of functions having Lipschitz continuous first partial derivatives. Pacific Journal of Mathematics. 1966; 16(1):1–3.
26. Nelson RB. Simplified calculation of eigenvector derivatives. AIAA Journal. Sep; 1976 14(9): 1201–1205.
27. Rao CR. Minimum variance and the estimation of several parameters. Proc Cambridge Phil Soc. 1946; 43:280–283.

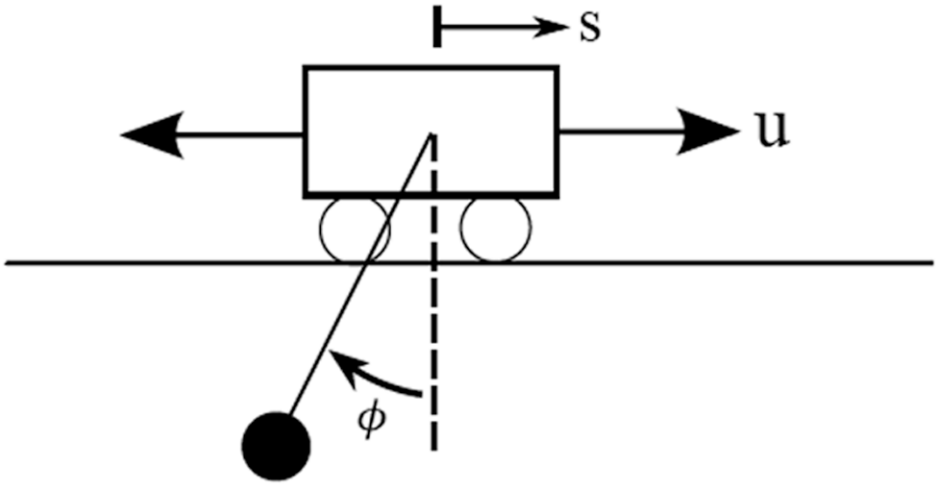

Fig. 1.
Cart-pendulum system

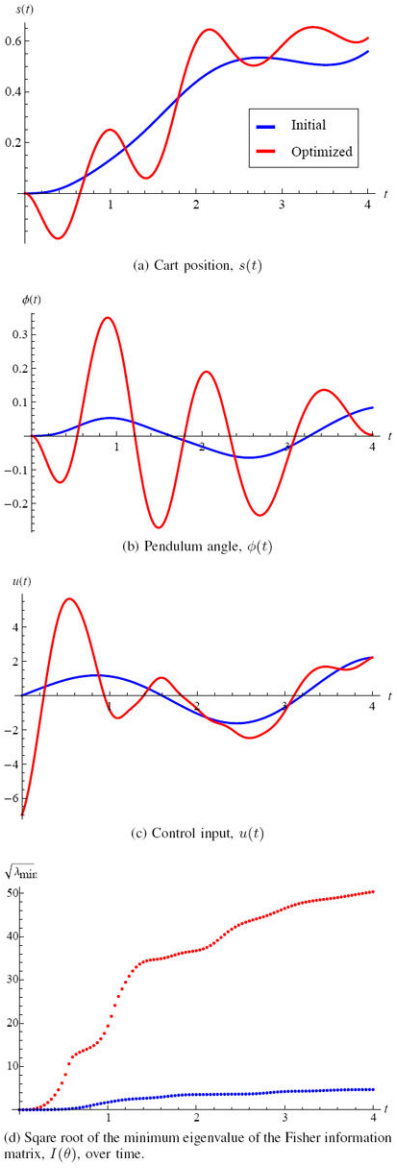

Fig. 2.

Comparisons of the trajectory before and after Fisher information optimization.

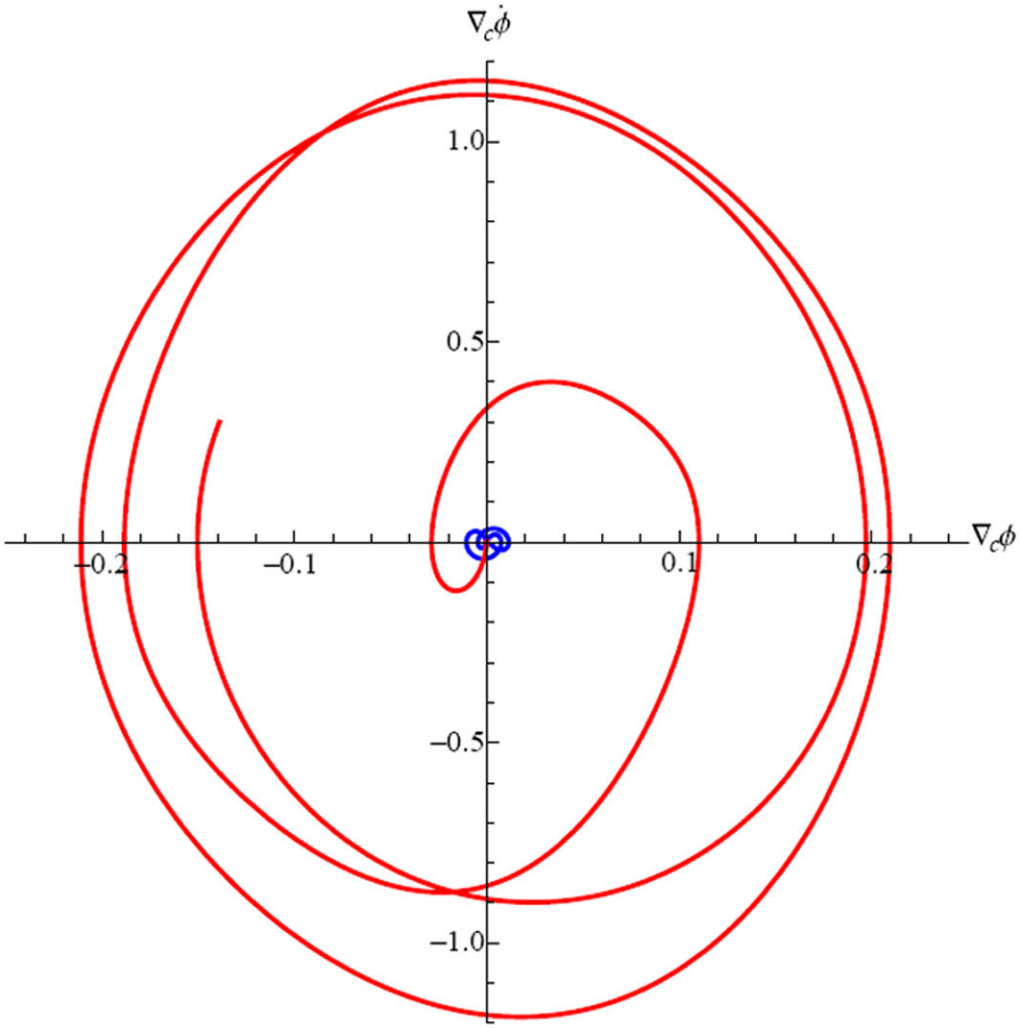

Fig. 3.

Phase plot of $\nabla_c\varphi(t)$ from initial (blue) and optimized (red) trajectories. Information is maximized by a trajectory that quickly causes the sensitivity w.r.t. parameters to increase.

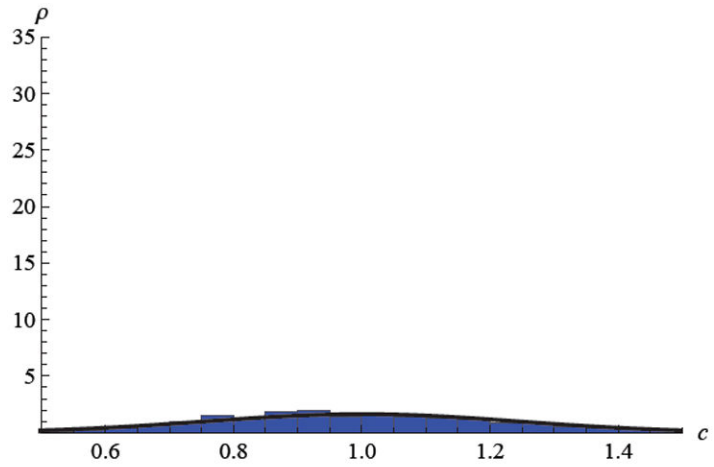

(a) Distribution using initial trajectory, $\sigma^2 = 0.0595$

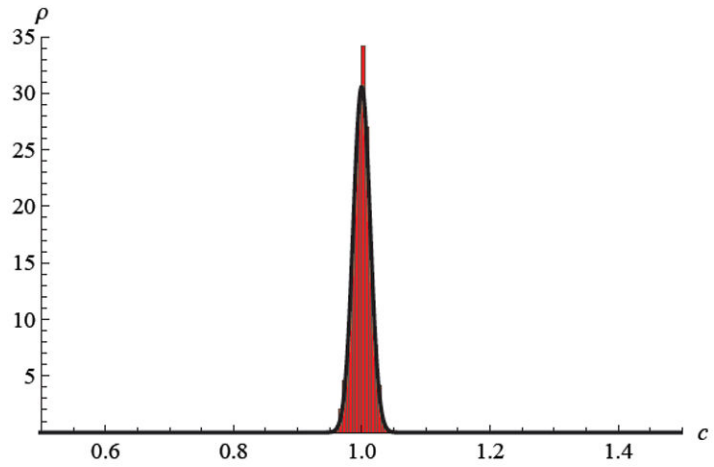

(b) Distribution using optimized trajectory, $\sigma^2 = 0.000170$

Fig. 4.
PDF histograms of the viscous friction coefficient, *c*.

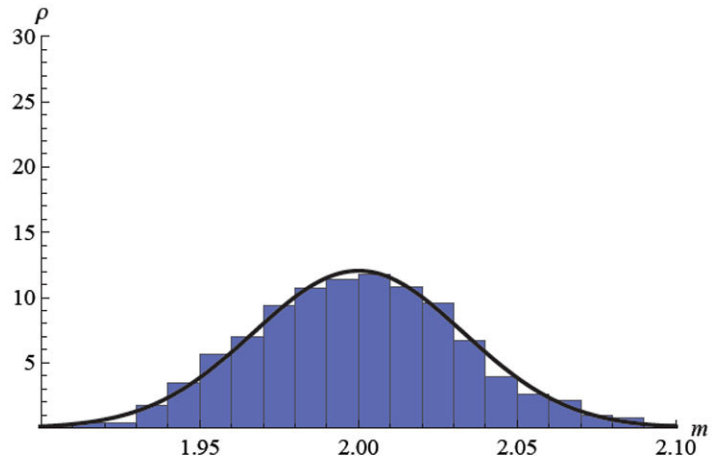

(a) Distribution using initial trajectory, $\sigma^2 = 0.00110$

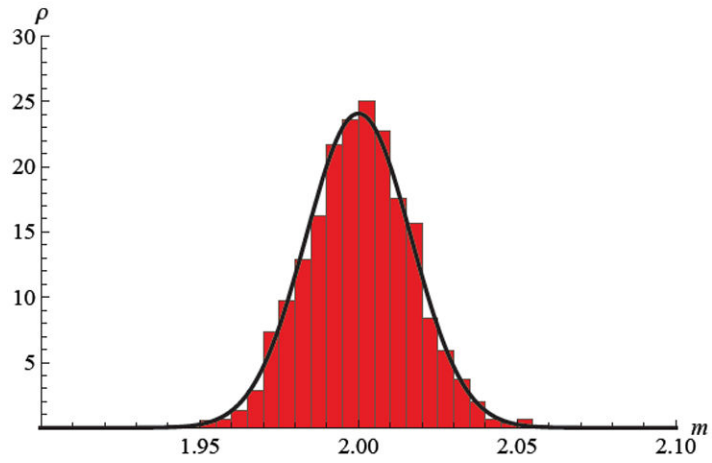

(b) Distribution using optimized trajectory, $\sigma^2 = 0.000275$

Fig. 5.
PDF histograms of the mass parameter, *m*.

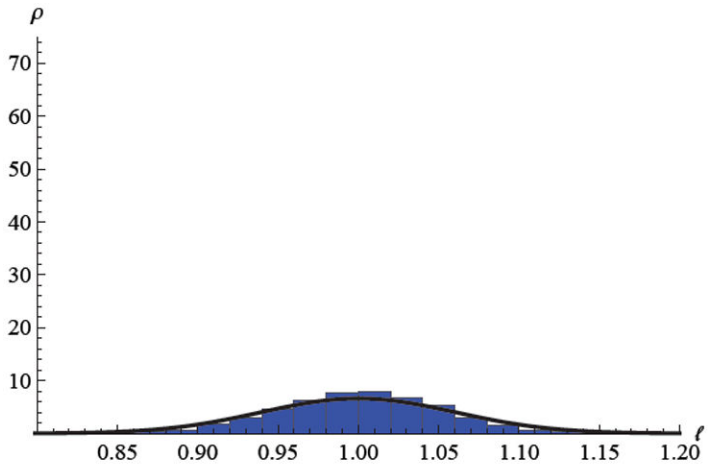

(a) Distribution using initial trajectory, $\sigma^2 = 0.00364$

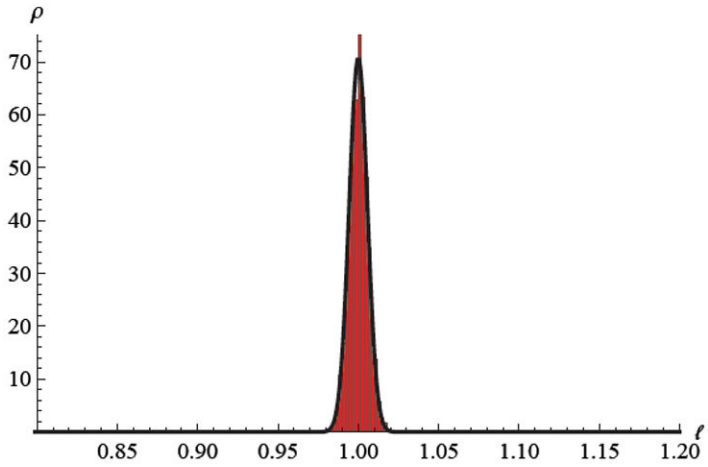

(b) Distribution using optimized trajectory, $\sigma^2 = 0.0000318$

Fig. 6.
PDF histograms of the length parameter, ℓ.

TABLE I

Optimization Cost

	λ_1	λ_2	λ_3	J
Initial	38.170	19.266	0.87185	1.1470
Optimized	16482.	928.51	101.24	0.0098775

TABLE II

Covariance and Fisher Information

Monte−Carlo Covariance

Initial:
$$\begin{bmatrix} 1.10 \times 10^{-3} & -1.51 \times 10^{-4} & 3.54 \times 10^{-4} \\ -1.51 \times 10^{-4} & 3.64 \times 10^{-3} & 4.92 \times 10^{-3} \\ 3.54 \times 10^{-4} & 4.92 \times 10^{-3} & 5.95 \times 10^{-2} \end{bmatrix}$$

Optimized:
$$\begin{bmatrix} 2.75 \times 10^{-4} & 8.68 \times 10^{-5} & 1.65 \times 10^{-4} \\ 8.68 \times 10^{-5} & 3.18 \times 10^{-5} & 6.21 \times 10^{-5} \\ 1.65 \times 10^{-4} & 6.21 \times 10^{-5} & 1.70 \times 10^{-4} \end{bmatrix}$$

Fisher Information Matrix

Initial:
$$\begin{bmatrix} 9.61 \times 10^{2} & 2.21 \times 10^{1} & -7.26 \\ 2.21 \times 10^{1} & 4.82 \times 10^{2} & -3.09 \times 10^{1} \\ -7.26 & -3.09 \times 10^{1} & 2.39 \times 10^{1} \end{bmatrix}$$

Optimized:
$$\begin{bmatrix} 3.16 \times 10^{4}. & -9.24 \times 10^{4}. & 2.45 \times 10^{3} \\ -9.24 \times 10^{4} & 3.84 \times 10^{5} & -5.02 \times 10^{4} \\ 2.45 \times 10^{3} & -5.02 \times 10^{4} & 2.33 \times 10^{4} \end{bmatrix}$$

TABLE III

Cramer-Rao Lower Variance Bounds

Initial:	$\begin{bmatrix} 1.04 \times 10^{-3} & -3.01 \times 10^{-5} & 2.78 \times 10^{-4} \\ -3.01 \times 10^{-5} & 2.26 \times 10^{-3} & 2.92 \times 10^{-3} \\ 2.78 \times 10^{-4} & 2.92 \times 10^{-3} & 4.57 \times 10^{-2} \end{bmatrix}$
Optimized:	$\begin{bmatrix} 2.63 \times 10^{-4} & 8.30 \times 10^{-5} & 1.51 \times 10^{-4} \\ 8.30 \times 10^{-5} & 2.98 \times 10^{-5} & 5.56 \times 10^{-5} \\ 1.51 \times 10^{-4} & 5.56 \times 10^{-5} & 1.47 \times 10^{-4} \end{bmatrix}$